Hydrodynamic analysis of the McIver toroid

J. N. Newman
Department of Ocean Engineering, MIT, Cambrdige, MA 02139, USA

Recently M. & P. McIver have shown, for certain floating bodies of finite dimensions, that a homogeneous solution of the linear water-wave radiation problem exists at a particular frequency ω_0 and corresponding wavenumber k_0. In two dimensions the body is generated by a pair of point sources separated by an odd multiple of a half wavelength. In three dimensions the body is a toroid, generated by a ring source of radius $r = c$, where $k_0 c$ is a zero of the Bessel function J_0. In both cases an interior free surface exists, similar to a 'moon pool'.

In discussions of two papers [1,2] at the last Workshop, questions were raised concerning (1) the local behavior of the added mass as $k \to k_0$ (damping was not mentioned explicitly), and (2) the conjecture that standard numerical methods would fail in the same limit. The present work is intended to address these issues, in the three-dimensional context, by applying the radiation/diffraction panel code WAMIT to the McIver toroid.

Geometrical construction

The first task is to consider the stream surface induced by a ring source of radius c. Nondimensional coordinates are used, with $c = 1$.

In [3] the velocity potential for a ring source is evaluated using analytic integration around the circle, but the remaining semi-infinite integral in wavenumber space is evaluated numerically with a truncation correction. A complementary procedure is followed here, using the subroutine for a point source based on the algorithms described in [4]. The Rankine singularity $1/R$ is replaced by elliptic integrals. The remaining part of the free-surface point source is integrated around the ring using an adaptive Gauss-Chebyshev quadrature. The wavenumber is fixed, with $k = j_{0,1} = 2.4048...$, the first zero of J_0. The streamlines, defined by the relation $\phi_r dz - \phi_z dr = 0$, are traced by Runge-Kutta integration. This procedure is easily extended to a submerged ring source, or to a finite fluid depth, with typical results shown in Figure 1. For the case of zero submergence in a fluid of infinite depth the results agree within graphical precision with the body contours shown in [3].

Radiation and diffraction analysis

The radiation and diffraction potentials on the body surface are evaluated from Green's theorem using the free-surface source potential as the Green function. The fluid depth is assumed infinite and the toroid is generated by rotating the outermost contour shown in Figure 1 about the vertical z-axis. Three different panelizations are used, with 512, 2048, and 8192 panels on the complete submerged surface. Except where otherwise noted, the irregular-frequency effects have been removed by imposing a Neumann condition on the plane $z = 0$ inside the body. Figure 2 shows the discretization with 2048 panels on the submerged surface and 1600 additional panels on $z = 0$ inside the body, giving a total of 3648 panels. Since two planes of symmetry are utilized, the total number of unknowns is reduced by a factor of 4.

The parameters evaluated include the heave added-mass, damping, and exciting-force coefficients, and the free-surface elevation at the center of the moon pool in the diffraction problem. The added-mass and damping coefficients are nondimensionalized by the factors ρc^3 and $\rho c^3 \omega$, respectively, where ρ is the fluid density and c the radius of the ring source. The exciting force is nondimensionalized by the factor $\rho g c^2 A$, where A is the incident-wave amplitude. The free-surface elevation is nondimensionalized by A. Approximately 200 closely-spaced wavenumbers have been used in the computations to define the details shown.

Figure 3 shows the added-mass and damping coefficients. Two sets of curves are included, where the effects of irregular frequencies are present (dashed) or removed (solid), to emphasize the distinction between the irregular frequencies and the physically relevant moon-pool resonance. The resonance, which occurs near the theoretical value $k = 2.4048$, is present in both sets of curves. The two extra singularities in the dashed curves are due to the irregular frequencies which exist in the vicinity of $k = 1.51$ and 2.81. Figure 4 compares the results based on the three different discretizations, in the vicinity of resonance. As $k \to k_0$ the number of panels must be increased to achieve a given accuracy. The peak of the damping coefficient is relatively narrow, and within this resonant regime the numerical results are not reliable as indicated by the negative damping peak for the intermediate discretization.

The precise wavenumber where resonance occurs depends on the number of panels, and differs according as whether or not the irregular-frequency removal algorithm is used. Figure 5 shows the wavenumber at which resonance occurs in each case, determined from the values of k at which the added mass passes through zero and the other parameters achieve their maximum amplitudes. As the number of panels increases both resonant wavenumbers tend to the correct theoretical value, with errors which appear to be inversely proportional to the number of panels.

Figure 6 shows the results from the diffraction solution including the moon-pool elevation and exciting force. The exciting force is evaluated both directly from integration of the diffraction pressure, and indirectly using the Haskind relations. Differences between the two methods are noticeable in the vicinity of the resonant wavenumber, where the diffraction exciting force has a very sharp peak and the width of the Haskind peak is somewhat greater. The exciting force and damping vanish at $k = 1.84....$

An explanation of the results in the resonant regime can be developed, along similar lines to the large added-mass and damping variations for bodies in channels, or submerged close to the free surface. Thus we assume that the solution matrix is singular, with a pole in the complex wavenumber plane. With the complex time factor $e^{i\omega t}$ the pole is generally above the real axis, but for the McIver toroid the pole is on the real axis at $k = k_0 = j_{0,1}$. Each discretized body is a perturbation of the toroid, with the pole shifted above the real axis by a small distance ϵ. As the number of panels tends to infinity, $\epsilon \to 0$. These assumptions imply that the added-mass and damping coefficients are approximated in the forms

$$A = \bar{A} + A_0 \frac{k - k_0}{(k - k_0)^2 + \epsilon^2}, \qquad B = \bar{B} + B_0 \frac{\epsilon}{(k - k_0)^2 + \epsilon^2}. \tag{1}$$

where $\bar{A}$ and $\bar{B}$ are bounded near $k = k_0$, $B_0 > 0$, and $A_0 = -B_0$. The numerical results in Figures 3-4 are consistent with these approximations. The singular behavior of the added mass occurs over a relatively broad band of wavenumbers, with the limiting form of the singularity proportional to $(k - k_0)^{-1}$, whereas the damping coefficient is similar to a delta-function. For an axisymmetric body the Haskind relations can be used to show that the damping coefficient is proportional to the square of the exciting force. Thus the singularity in the exciting force is weaker than for the damping coefficient, but with the same narrow width $O(\epsilon)$. Assuming that the diffraction pressure is singular in the same manner, the amplitude of the free-surface elevation in the moon pool is similar. These conjectures are consistent with the results shown in Figure 6.

Further details are given in a paper which has been submitted for publication in the Journal of Engineering Mathematics Special Edition on Ocean Mechanics. I am indebted to Dr. C.-H. Lee and Dr. P. McIver for substantive discussions and assistance.

References

1. M. McIver, Resonance in the unbounded water wave problem. *Proceedings of the 12th IWWWFB*, Carry-le-Rouet (1996) 177-181.

2. P. McIver & N. Kuznetsov. On uniqueness and trapped modes in the water-wave problem for a surface-piercing axisymmetric body. *Proceedings of the 12th IWWWFB*, Carry-le-Rouet (1996) 183-187.

3. P. McIver and M. McIver, Trapped modes in an axisymmetric water-wave problem. *Quart. J. Mech. Appl. Math.* 50 (1997) 165-178.

4. J. N. Newman, Approximation of free-surface Green functions. In: P. A. Martin and G. R. Wickham (eds.), *Wave Asymptotics*. Cambridge, UK: Cambridge University Press (1992) 107-135.

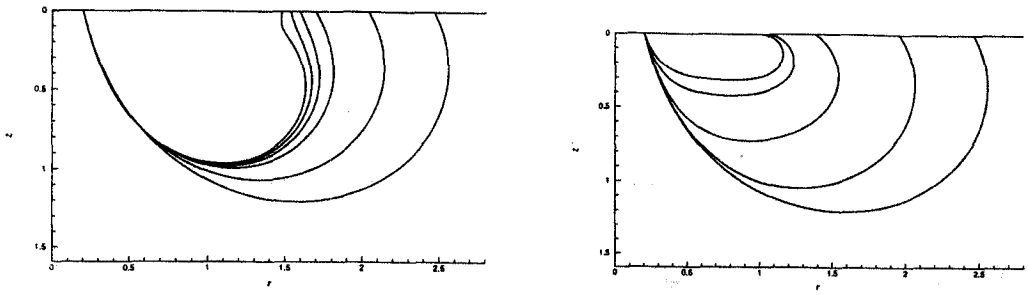

Figure 1: Contours of cross-sections generated by a ring source. In the left figure the source is submerged at the depths $\zeta = 0, 0.2, 0.25, 0.26, 0.265, 0.269$, respectively, proceeding from the outermost to the innermost section; the fluid depth is infinite. In the right figure the source is in the free surface and the fluid depths are $h = \infty, 2.0, 1.0, 0.5, 0.36$. In both cases the inner radius is fixed at 0.2 .

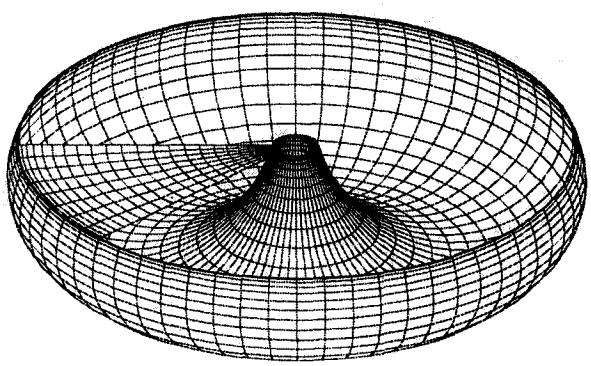

Figure 2: Perspective view of the body panelization, generated from the outermost contour in Figure 2, with 32 cosine-spaced segments along the contour and 64 equally-spaced azimuthal segments, giving a total of 2048 panels on the submerged surface. The 45°-sector of the interior free surface shows the additional panels used for the removal of irregular-frequency effects.

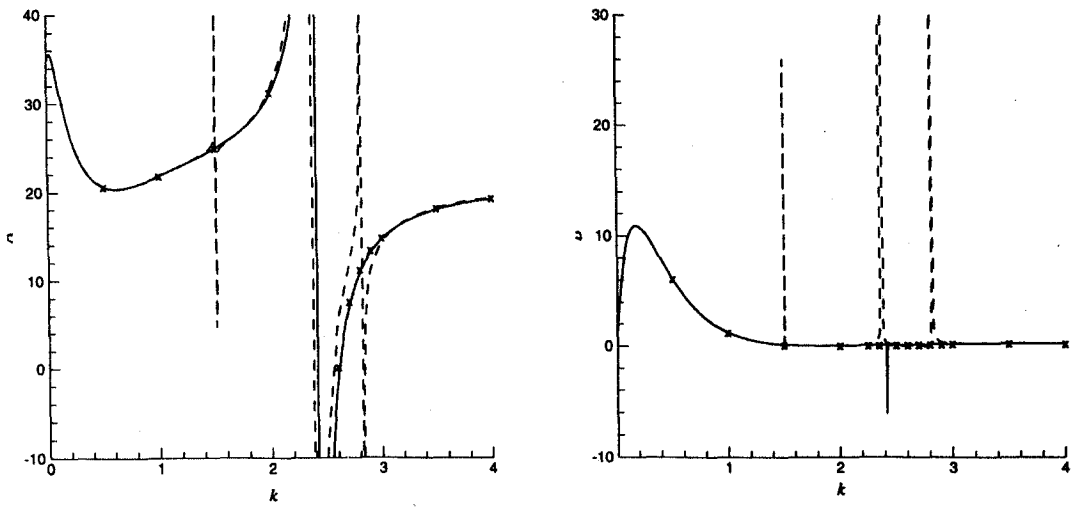

Figure 3: Heave added mass (left) and damping (right). The dashed curves include irregular-frequency effects, which are removed in the other results. The dashed and solid curves denote computations using 2048 panels on the body and '×' represents computations with 8192 panels.

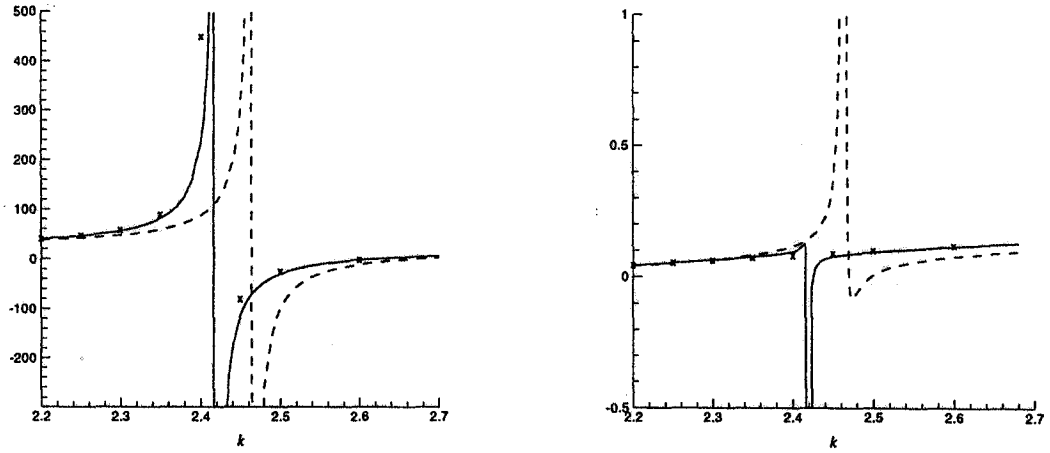

Figure 4: Added mass (left) and damping (right) in the vicinity of resonance, showing the convergence of results using 512 (dashed curve), 2048 (solid curve), and 8192 (×) panels on the submerged body surface.

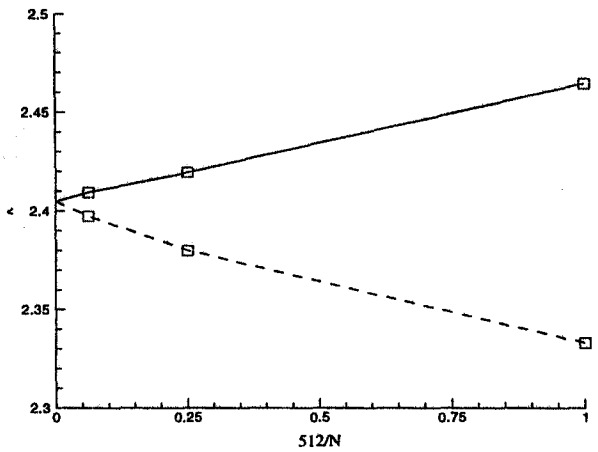

Figure 5: The resonant wavenumber for each discretization, showing the convergence to the theoretical limit $j_{0,1} = 2.4048....$ The dashed curve is based on computations including the irregular-frequency effects.

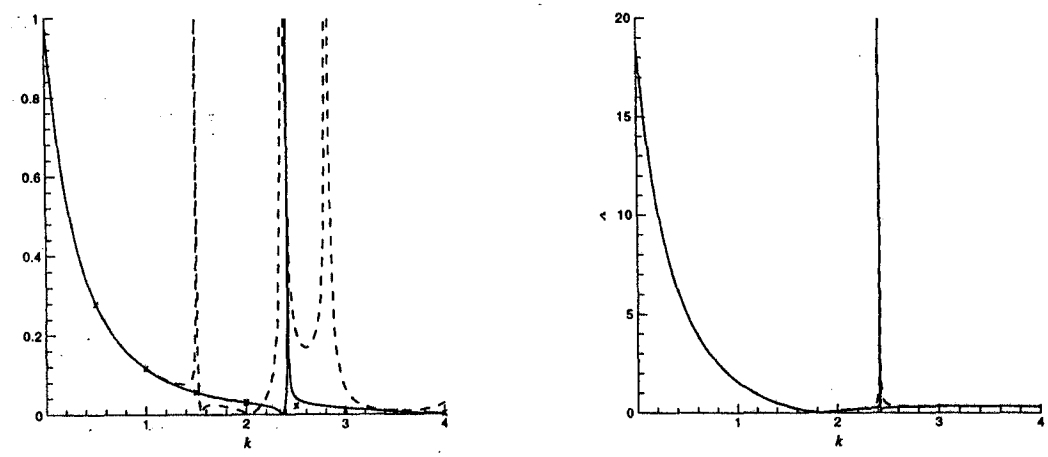

Figure 6: Free-surface elevation in the moon pool (left) and heave exciting force (right) for the body fixed in incident waves. The dashed curve in the left figure includes irregular-frequency effects, and the marks '×' represent computations with 8192 panels. The dashed curve in the right figure represents the exciting force based on the Haskind relations.